Nonlinear microwave response of MgB$_2$ thin films

To cite this article: James C Booth *et al* 2003 *Supercond. Sci. Technol.* **16** 1518

View the article online for updates and enhancements.

Nonlinear microwave response of MgB$_2$ thin films*

James C Booth[1], K T Leong[1], Sang Young Lee[2], J H Lee[2], B Oh[3,5], H N Lee[3] and S H Moon[4]

[1] National Institute of Standards and Technology, Mail Stop 814-03, 325 Broadway, Boulder, CO, 8035, USA
[2] Department of Physics, Konkuk University, 1 Hwayang-dong, Kwangjin-gu, Seoul, 143-701, Korea
[3] D&M Lab, LG Electronics Institute of Technology, 16 Woomyeon-dong, Seocho-gu, Seoul, 137-724, Korea
[4] School of Material Science and Engineering, College of Engineering, Seoul National University, San 56-1, Shillim-dong, Kwanak-gu, Seoul, 151-742, Korea

Abstract

Thin films of the recently discovered superconductor MgB$_2$ show promise for a number of different electronic applications. In order to evaluate the suitability of this new material for communication applications at microwave frequencies, we have measured both the linear and nonlinear microwave response of *ex situ* fabricated thin films of MgB$_2$ on sapphire substrates patterned into coplanar-waveguide (CPW) transmission lines. Linear measurements yield the surface resistance and absolute value of the penetration depth, as well as the characteristic impedance of our MgB$_2$ transmission lines. The nonlinear response of the same transmission lines was then measured by harmonic generation. Assuming that the measured nonlinear response is due to kinetic inductance effects, we were able to directly determine the relevant pair-breaking current density in our MgB$_2$ thin films by combining results from our linear and nonlinear measurements. Because the resulting pair-breaking current density is an intrinsic material property independent of sample geometry, we can quantitatively compare the nonlinear responses of MgB$_2$ thin films and YBa$_2$Cu$_3$O$_{7-\delta}$ (YBCO) thin films at comparable reduced temperatures. We find that for sufficiently low reduced temperatures the pair-breaking current density in MgB$_2$ thin films rivals that in YBCO.

1. Introduction

The microwave surface resistance of MgB$_2$ thin films has been shown to be comparable to that of YBCO thin films at low reduced temperatures, with values of 80 $\mu\Omega$ observed in MgB$_2$ films at 20 K and 8.5 GHz [1]. This suggests that MgB$_2$ films may be useful for passive microwave devices operated at temperatures around 20 K. A key property of superconducting films for microwave frequency applications is their nonlinear response, since a large nonlinear response will produce undesirable intermodulation products, which can mitigate the benefits of superconducting devices for telecommunication applications. It is therefore important to accurately characterize the nonlinear response of this newest superconductor at microwave frequencies.

Although the nonlinear response of MgB$_2$ films has been measured previously [2, 3], the results of nonlinear characterization measurements are often applicable only to the specific geometry that has been measured, making it difficult to compare the nonlinear response of different samples or materials, or to predict nonlinear effects in arbitrary device geometries. To overcome this limitation of nonlinear characterization, we have combined the results of our nonlinear measurements with a detailed linear characterization of the thin-film sample in order to yield a measure of nonlinear

response that is device independent, and that can be used to quantitatively compare the nonlinear response of different materials. To accomplish this, we assumed a simple model for the nonlinear response of our superconducting MgB$_2$ thin films that is based on a current-dependent superconductor penetration depth. We then used linear transmission-line measurements of the absolute value of the penetration depth as well as the characteristic impedance of our CPW transmission lines to extract a value for the pair-breaking current density from nonlinear harmonic-generation experiments on the same transmission-line structures. We use a simple quadratic form for the nonlinear penetration depth that is appropriate for describing current-induced pair-breaking in superconducting materials [4], and which has been successfully applied to describe nonlinear effects in YBa$_2$Cu$_3$O$_{7-\delta}$ (YBCO) thin films [5, 6]. We demonstrate the utility of this approach by directly comparing the extracted nonlinear pair-breaking current density of MgB$_2$ films with that of YBCO films at comparable reduced temperatures.

2. Nonlinear measurements

MgB$_2$ thin films on c-cut sapphire substrates were prepared in an *ex situ* process by annealing a pure boron film in a magnesium-rich environment within a sealed quartz tube [7]. The resulting thin films were approximately 350 nm thick and were 20×20 mm^2 in area. Surface ion milling has been shown to improve the microwave surface resistance [8], and also to aid in passivation for thin films of MgB$_2$. Such surface-ion-milling procedures have been applied to the MgB$_2$ films grown by the above method. Temperature-dependent measurements of the surface impedance were performed on the unpatterned MgB$_2$ samples [9], after which the films were patterned into coplanar-waveguide (CPW) transmission lines and resonators by optical photolithography and Ar ion milling. Contact pads were formed by deposition of Ti/Au by electron-beam evaporation. After processing was completed, our patterned chip contained a number of different CPW transmission lines of different lengths and cross-sections, as well as resonators and dc measurement structures.

We determined the nonlinear response of *ex situ* prepared films of MgB$_2$ on sapphire substrates using harmonic-generation measurements at a fundamental frequency of 4.2 GHz in patterned CPW transmission lines, as discussed in [2]. Figure 1 shows an example of such measurements for a 22 μm linewidth CPW transmission line fabricated from a MgB$_2$ thin film, where the output at the fundamental and third-harmonic frequencies is plotted as a function of the magnitude of the incident signal. The third harmonic displays a slope of 3 on the log–log plot over much of the input power range, and the third-order intercept point IP_3 is defined as the intersection of a line of slope 3 fit to the third harmonic with a line of slope 1 fit to the fundamental. As long as the third-harmonic signal increases with incident power with slope 3, the third-harmonic response can be completely described by specifying simply the third-order intercept point (in fact, any intercept on the line of slope 3 will suffice). Figure 2 shows the measured third harmonics for the same transmission line at different temperatures, demonstrating that the third harmonics become smaller as the temperature is decreased. This indicates less
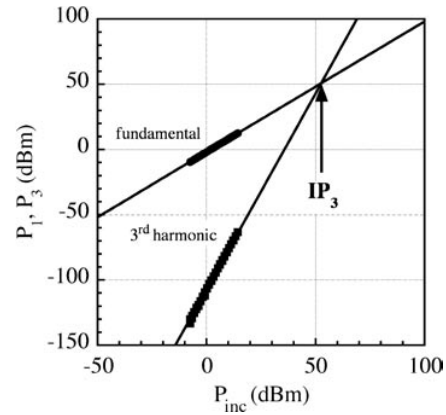
Figure 1. Transmitted power in the fundamental and third harmonic as a function of incident power in the fundamental for a 2.7 mm long, 22 μm linewidth MgB$_2$ CPW transmission line at 30 K. The intercept of a line of slope 3 fit to the third-harmonic data with a line of slope 1 fit to the fundamental data defines the third-order intercept IP_3.
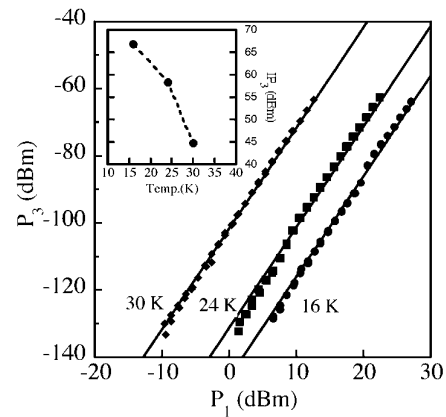
Figure 2. Third-harmonic generation at different temperatures from a 2.7 mm long CPW transmission line fabricated from a MgB$_2$ thin film. The inset shows the resulting third-order intercept IP_3 as a function of temperature.

nonlinear behaviour as the temperatures decreases, resulting in larger values for the third-order intercepts, as shown in the inset.

While the data in figures 1 and 2 provide valuable information regarding the nonlinear response of MgB$_2$ patterned devices at microwave frequencies, the third-order intercepts in general depend explicitly on the geometry of the device under test [5]. This is demonstrated by figure 3, which shows the measured third-order intercepts for transmission lines of different length fabricated on the same MgB$_2$ thin-film sample. These data display the same temperature dependence as was shown in figure 2, but also show that the third-order intercepts decrease as the transmission line increases in length. This demonstrates that it is difficult to directly compare the nonlinear response described here with measurements of the nonlinear response in other MgB$_2$ thin-film devices having different geometries, or in general to predict the nonlinear response of an actual microwave device of arbitrary geometry fabricated from thin films of MgB$_2$.
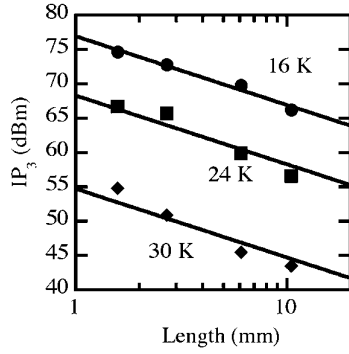
Figure 3. Third-order intercept IP_3 as a function of transmission-line length at three different temperatures. The solid lines show a fit to a $1/\ell$ length dependence.

3. Nonlinear penetration depth

In order to model nonlinear effects in high-temperature superconductors, we assumed a current-dependent penetration depth of the form [4]

$$\lambda^2(T, J) = \lambda^2(T, 0)\left[1 + \left(\frac{J}{J_2(T)}\right)^2\right], \qquad (1)$$

where J is the current density, $\lambda(T, 0)$ is the linear penetration depth at temperature T and zero current, and $J_2(T)$ is a current-density scale that quantifies the strength of the nonlinearity of the penetration depth. Equation (1) is appropriate for describing current-induced depairing [10], for which $J_2(T)$ corresponds to the depairing current density. Mutual inductance measurements of the current-density-dependent penetration depth in YBCO thin films at audio frequencies [11] demonstrate that equation (1) accurately describes the nonlinear penetration depth for YBCO, at least for temperatures around 76 K and for current densities well below the critical-current density.

The nonlinear penetration depth given in equation (1) results in a transmission-line inductance per unit length $L(I)$ that depends quadratically [6] on the transmission-line current I: $L(I) = L_0 + L'I^2$, where L_0 is the linear contribution to the inductance, and L' is the coefficient of the nonlinear contribution to the inductance. From such a nonlinear inductance per unit length, it is straightforward to calculate the voltage, and hence the power, generated at the frequency of the third harmonic [6]. For our coplanar-waveguide transmission lines, we obtained the following expression for the third-harmonic signal P_3 as a function of the fundamental signal P_1,

$$\log P_3 = -2\log IP_3 + 3\log P_1, \qquad (2)$$

where IP_3 is the third-order intercept point, which is given by the expression

$$IP_3 = \frac{2Z_0^2 J_2^2}{\mu_0\omega\lambda^2\Gamma'\ell}. \qquad (3)$$

In equation (3), Z_0 is the characteristic impedance of the transmission line, ω is the angular frequency, ℓ is the length of the transmission line, and Γ' is a geometric factor given by

$$\Gamma' = \frac{\int J^4\,dS}{(\int J\,dS)^4}. \qquad (4)$$

In equation (4) the integration is performed over the cross-section of the planar transmission line. In order to evaluate Γ' in equation (4), we need to know the distribution of the current density across the cross-section of our CPW transmission lines. In what follows, we describe how we obtained the characteristic impedance as well as the total inductance per unit length of our CPW transmission lines using detailed linear measurements. Once this is accomplished, the geometric factor Γ' as well as the absolute value of the penetration depth can be obtained from a numerical calculation of the transmission-line inductance developed by Sheen [12], also described below.

4. Transmission-line parameters

From equations (3) and (4) it is clear that it is possible to determine the pair-breaking current density J_2 from measurements of the third-order intercept IP_3 provided that the characteristic impedance and the penetration depth are known. We employed wafer-probe measurements of our CPW transmission lines to determine these quantities at the temperature of interest for our nonlinear measurements. Multiline TRL calibrations yield the propagation constant as a function of frequency $\gamma(\omega)$ for our CPW transmission lines [13], shown in figure 4(*a*), while the calibration comparison method [14] is used to determine the characteristic impedance $Z_0(\omega)$, shown in figure 4(*b*). These quantities were determined for the same transmission lines used for our nonlinear measurements, and can be combined to yield the distributed resistance, inductance, capacitance, and conductance (R, L, C and G, respectively), all per unit length.

The inductance per unit length of our CPW transmission lines, shown in figure 5 as a function of frequency, contains a contribution from the kinetic inductance of the MgB_2 thin film. We used the method of Sheen *et al* [12] to numerically calculate, for our specific CPW transmission-line geometry, the inductance per unit length as a function of the superconducting penetration depth, the result of which is shown in the inset to figure 6. We can then use these calculations to extract the penetration depth of our MgB_2 thin films from the measured value for the inductance per unit length determined by our multiline TRL calibrations. The values for the penetration depth extracted from the measured inductance per unit length shown in figure 5 are plotted in figure 6. Also shown in figure 6 are the values for the penetration depth extracted from transmission lines of different cross-sections patterned onto the same thin-film sample. The solid line in figure 6 represents the change in the penetration depth determined from the frequency shift of a patterned CPW resonator. These different determinations of the penetration depth from patterned device measurements are consistent with one another, and the value obtained for the penetration depth at low temperature ($\lambda(16\text{ K}) \sim 100$ nm) is also in good agreement with in-plane penetration depth determinations for MgB_2 from muon spin relaxation [15] ($\lambda(0) \sim 100$ nm), tunnel diode oscillator measurements [16] ($\lambda(0) \sim 120$ nm), and temperature-dependent fits to microwave resonator frequency shift data [17] ($\lambda(0) \sim 105$ nm). Once we have determined the
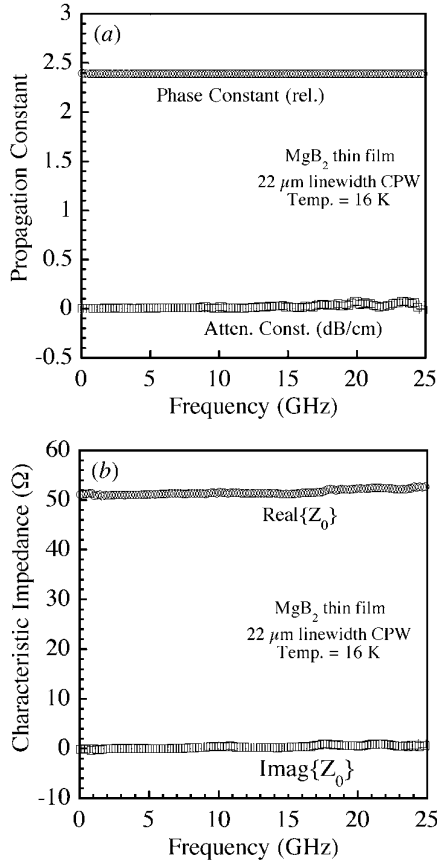
Figure 4. Measured (*a*) propagation constant and (*b*) characteristic impedance at 16 K for a 22 μm linewidth CPW transmission line fabricated from a MgB$_2$ thin film. The phase constant is relative to the speed of light, while the attenuation constant is in dB cm^{-1}.
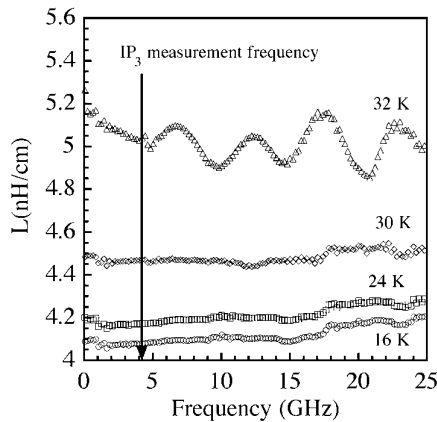
Figure 5. Measured transmission-line inductance per unit length as a function of frequency at four different temperatures for a 22 μm linewidth CPW transmission line fabricated from a MgB$_2$ thin film.

penetration depth for our MgB$_2$ samples, we can determine the distribution of the current density over the cross-sectional area of our transmission lines using the same numerical calculation [12].
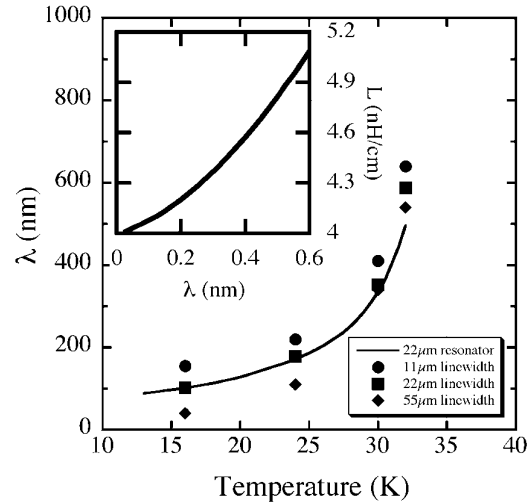
Figure 6. Penetration depth for a MgB$_2$ thin film as a function of temperature determined by multiline TRL measurements of CPW transmission lines. The solid line shows the change in penetration depth determined from measurements of the frequency shift of a 22 μm linewidth CPW resonator. The inset shows the calculated inductance per unit length as a function of penetration depth, from which the penetration depth is obtained using the measured data shown in figure 5.
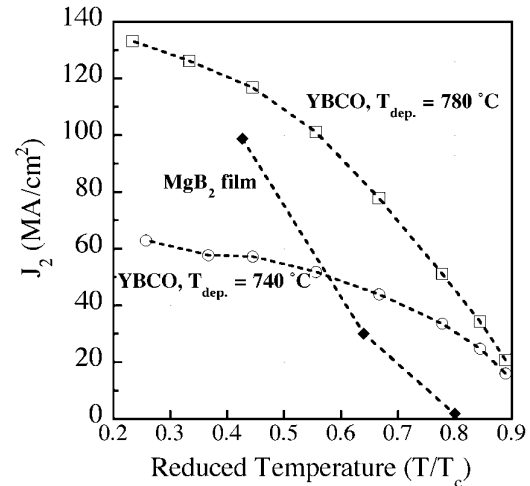
Figure 7. Pair-breaking current density J_2 as a function of reduced temperature for a MgB$_2$ thin film, and also for two YBCO thin films grown by laser ablation at two different deposition temperatures.

5. Experimental results

The above method allows us to determine all of the relevant transmission-line and material parameters for our MgB$_2$ transmission lines that are necessary to calculate the pair-breaking current density J_2 from our third-harmonic measurements. The data in figure 1 demonstrate that the third harmonic increases with slope 3, as predicted by equation (2), and the extracted third-order intercepts IP_3 shown in figure 3 confirm the transmission-line length dependence given in equation (3) [5]. The pair-breaking current density extracted from these measurements is shown in figure 7 as a function of

reduced temperature, along with the same quantity extracted from similar measurements on two different YBCO thin films grown at different deposition temperatures [18] (for the YBCO thin films, the penetration depth was measured separately). It is interesting to note that for temperatures less than $0.5T_c$, the pair-breaking current density in MgB_2 is similar in magnitude to that observed for YBCO thin films.

6. Conclusions

We have measured the nonlinear response of MgB_2 thin films in CPW transmission lines as a function of temperature. Using detailed linear characterization of the patterned transmission lines under test, we have successfully extracted the pair-breaking current density for this material. The pair-breaking current density quantifies the nonlinear response in a manner independent of geometry, and can be used to predict the nonlinear response of arbitrary microwave devices. Using this quantity, we have shown that the nonlinear effects in MgB_2 thin films are similar in magnitude to those in YBCO thin films, reflecting perhaps a similar origin for nonlinear effects in these two superconducting materials.

Acknowledgments

References

[1] Lee S Y *et al* 2003 *IEEE Trans. Appl. Supercond.* **13** 3595
[2] Booth J C *et al* 2003 *IEEE Trans. Appl. Supercond.* **13** 3590
[3] Lamura G *et al* 2003 *Appl. Phys. Lett.* **82** 4525
[4] Dahm T and Scalapino D J 1997 *J. Appl. Phys.* **81** 2002
[5] Booth J C, Beall J A, Rudman D A, Vale L R and Ono R H 1999 *J. Appl. Phys.* **86** 1020
[6] Booth J C, Vale L R, Ono R H and Claassen J H 2001 *J. Supercond.: Inc. Novel Magnetism* **14** 65
[7] Moon S H *et al* 2001 *Appl. Phys. Lett.* **79** 2429–31
[8] Lee S Y *et al* 2001 *Appl. Phys. Lett.* **79** 3299
[9] Lee S Y *et al* 2003 *IEEE Trans. Appl. Supercond.* **13** 3585
[10] Hammond R B *et al* 1998 *J. Appl. Phys.* **84** 5662
[11] Claassen J H *et al* 1999 *Appl. Phys. Lett.* **74** 4023
[12] Sheen D M *et al* 1991 *IEEE Trans. Appl. Supercond.* **1** 108
[13] Marks R B 1991 *IEEE Trans. Microwave Theory Tech.* **39** 1205
[14] Williams D F and Marks R B 1992 *38th ARFTG Conf. Digest* pp 68–81
[15] Niedermayer Ch, Bernhard C, Holden T, Kremer R K and Ahn K 2002 *Phys. Rev.* B **65** 094512
[16] Manzano F *et al* 2002 *Phys. Rev. Lett.* **88** 047002
[17] Jin B B *et al* 2002 *Phys. Rev.* B **66** 104521
[18] Booth J C *et al* 1999 *IEEE Trans. Appl. Supercond.* **9** 4176